[arXiv:2207.10378]

Cosmological prior for the J-factor estimation of dwarf spheroidal galaxies

Shunichi Horigome, Kohei Hayashi, Shinichiro Ando

Kavli IPMU (WPI)

NuDM-2022 26 September 2022

Cosmological prior for the J-factor estimation of dwarf spheroidal galaxies

- Dwarf spheroidal galaxies (dSph) play important roles for dark matter detection but their dark matter halo profiles have large uncertainties
- For the halo profile estimation of dSphs, we apply two **cosmological priors**:
  - Satellite prior: constraint distribution of halo parameter based on a structure formation model
  - Stellar-to-halo mass relation prior: empirical relation between stellar mass and halo mass
- The cosmological priors are useful to decrease the uncertainty in the estimation and give a better understanding of dSphs

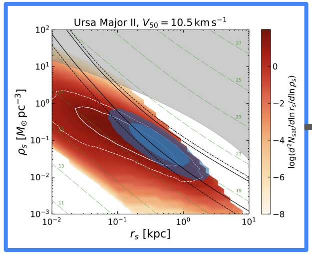

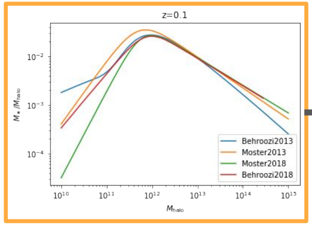

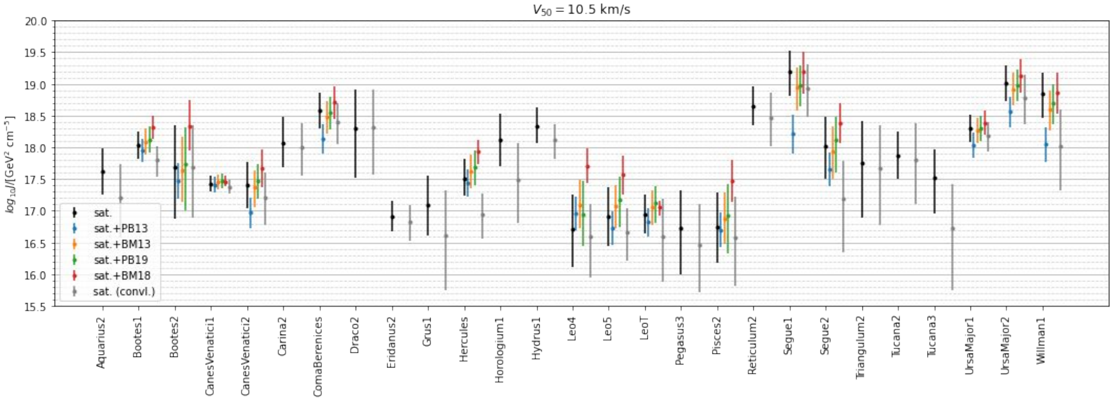

Introduction

dSphs and DM detection

- Dwarf spheroidal galaxies (dSphs)
  - Containing large amount of DM
  - Good candidates for the indirect detection of the WIMP DM

e.g. Fornax dSph

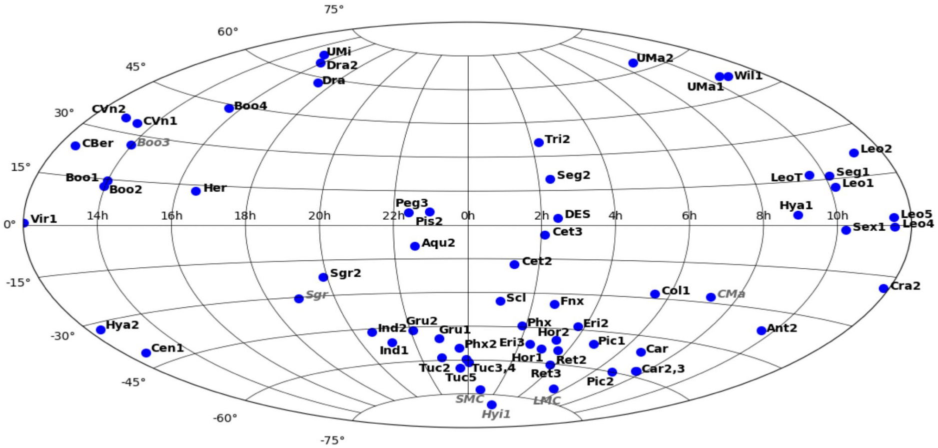

McConachie et al. [2007.05011]

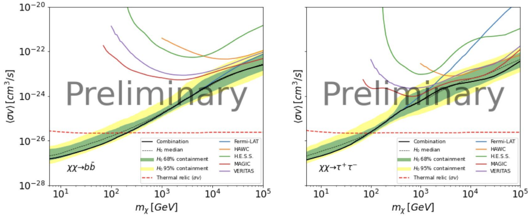

Armard et al. [2108.13646]

dSphs and DM detection

- The sensitivity of the indirect detection depends on the DM profile of dSph
  - Indirect detection: DM annihilation into SM particles (gamma-ray etc.)
    - Signal flux from dSphs:

$$\Phi(E, \Delta\Omega) = \left[\frac{C\langle\sigma v\rangle}{4\pi m_{\mathrm{DM}}^2} \sum_f b_f \left(\frac{dN_\gamma}{dE} \right)_f \right] \times J(\Delta\Omega)$$

$$J(\Delta\Omega) = \left[\int_{\Delta\Omega} \mathrm{d}\Omega \int_{\mathrm{l.o.s.}} \mathrm{d}l\, \rho_{\mathrm{DM}}^2(l,\, \Omega) \right]$$

How to estimate DM density profile

- dSph member stars move in the gravitational potential yielded by DM mass density
- Velocity of member stars is observed by spectroscopic telescope

spectroscopic observation

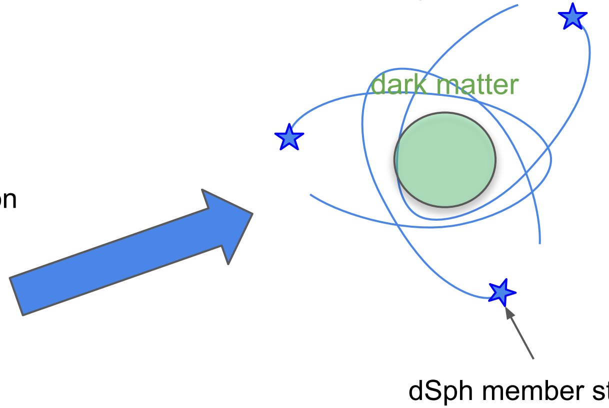

e.g. Stellar velocity distibution of the Sculptoir dSph

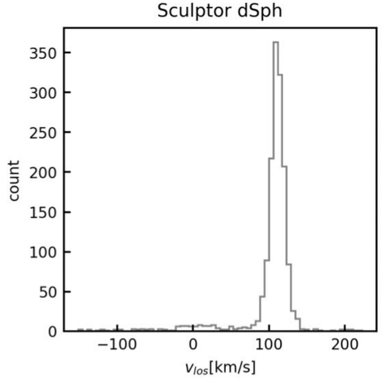

J-factor uncertainty

- J-factor has large uncertainty
  - Limited number of dataset
    - Classical: O(100)
    - Ultrafaint: O(10)

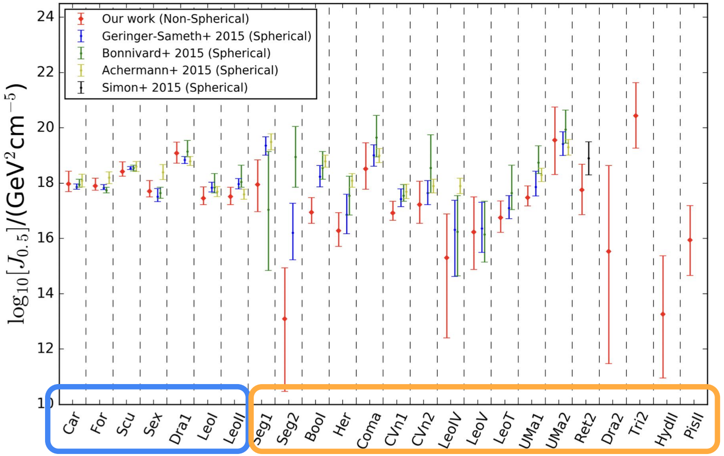

Hayashi et al. [1603.08046]

- We use "cosmological prior" to improve the accuracy

Our analysis:
Estimation with cosmological prior

Jeans analysis

- Jeans equation: kinematical equation of dSph systems
  - Assumption: sphericity

$$\frac{1}{\nu_*(r)}\frac{\partial(\nu_*(r)\sigma_r^2(r))}{\partial r}+\frac{2\beta(r)\sigma_r^2(r)}{r}=-\frac{GM_{\mathrm{DM}}(r)}{r^2}$$

(stellar distribution & velocity dispersion) ~ (inner dark matter mass)

- Observable: line-of-sight velocity dispersion (R-dependent)

$$\sigma_{\mathrm{los}}^2(R)=\frac{2}{\Sigma(R)}\int_R^\infty \mathrm{d}r\left(1-\beta(r)\frac{R^2}{r^2}\right)\frac{\nu(r)\sigma_r^2(r)}{\sqrt{1-R^2/r^2}}$$

- Models:
  - Stellar profile: Plummer model
  - DM profile: truncated NFW model
  - Anisotropy profile: constant model

Likelihood

- Likelihood function

$$\mathscr{L}(\Theta) = \prod \mathcal{N}[v_i; v_{\mathrm{dSph}}, \sigma^2_{\mathrm{los}}(R_i) + \delta\sigma_i^2],$$

- Posterior probability

$$P(\Theta|D) = \frac{\mathscr{L}(\Theta)\pi(\Theta)}{\int \mathrm{d}\Theta\, \mathscr{L}(\Theta)\pi(\Theta)},$$

  - $\pi(\Theta)$: **prior**

$$\pi = \begin{cases} \pi_{\mathrm{photo.}} & \text{(without any cosmological priors)} \\ \pi_{\mathrm{photo.}}\pi_{\mathrm{sat.}} & \text{(satellite prior only)} \\ \pi_{\mathrm{photo.}}\pi_{\mathrm{sat.+SHMR}} & \text{(satellite \& SHMR prior)} \end{cases}$$

Priors (1/3)

- Photometry prior: for stellar distribution
    - half-light radius determined by phtometric observation

Name	$\log_{10} r_e/[\mathrm{pc}]$
Aquarius 2	2.094 ± 0.078
Boötes 1	2.204 ± 0.015
Boötes 2	1.523 ± 0.068
CanesVenatici 1	2.529 ± 0.017
CanesVenatici 2	1.732 ± 0.086
Carina	2.392 ± 0.005
Carina 2	1.870 ± 0.045
ComaBerenices	1.757 ± 0.029
Draco	2.256 ± 0.005
Draco 2	1.121 ± 0.182
Eridanus 2	2.196 ± 0.046
Fornax	2.849 ± 0.003
Grus 1	1.267 ± 0.459
Hercules	2.080 ± 0.042
Horologium 1	1.488 ± 0.097
Hydrus 1	1.727 ± 0.030
Leo 1	2.353 ± 0.004
Leo 2	2.217 ± 0.005
Leo 4	2.013 ± 0.053
Leo T	2.125 ± 0.051
Leo 5	1.571 ± 0.181
Pegasus 3	1.616 ± 0.158
Pisces 2	1.678 ± 0.072
Reticulum 2	1.495 ± 0.018
Sagittarius	3.191 ± 0.020
Sculptor	2.359 ± 0.004
Segue 1	1.295 ± 0.062
Segue 2	1.528 ± 0.038
Sextans 1	2.538 ± 0.004
Triangulum 2	1.096 ± 0.134
Tucana 2	2.212 ± 0.073
Tucana 3	1.640 ± 0.058
UrsaMajor 1	2.176 ± 0.024
UrsaMajor 2	1.930 ± 0.022
UrsaMinor	2.434 ± 0.006
Willman 1	1.304 ± 0.045

Priors (2/3)

- Satellite prior [1803.07691, 2002.11956]
  - Accretion of subhalo: extended Press-Schechter (EPS) formalism
  - Tidal stripping effect: semi-analytical subhalo model calibrated by N-body simulation

$$\dot{m}(z) = -A \frac{m(z)}{\tau_{\rm dyn}(z)} \left[\frac{m(z)}{M(z)} \right]^{\zeta}$$

$$P_{\rm sat}(r_s, \rho_s, r_t) \propto \frac{d^3 N_{\rm sat}}{dr_s d\rho_s dr_t} = \frac{d^3 N_{\rm sh}}{dr_s d\rho_s dr_t} P_{\rm form}(V_{\rm peak}).$$

$$P_{\rm form}(V_{\rm peak}) = \frac{1}{2}\left[1 + {\rm erf}\left(\frac{V_{\rm peak} - V_{50}}{\sqrt{2}\sigma}\right)\right]$$

V_peak: maximum circular velocity
V_50 = 10.5 km/s or 18 km/s

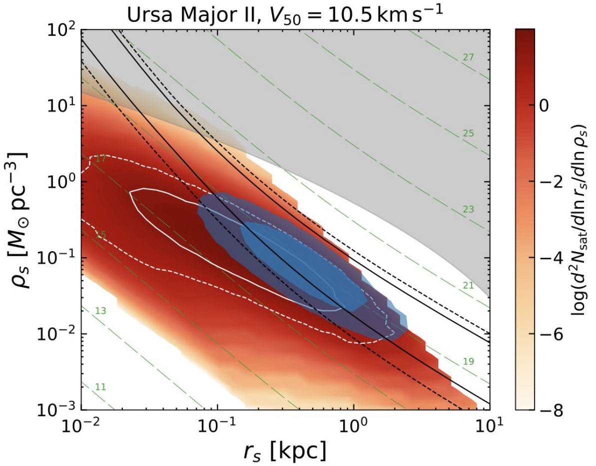

Ando+(2020) [2002.11956]

Priors (3/3)

- The stellar-to-halo mass relation (SHMR)
  - empirical relation between the stellar and DM halo mass of galaxies: M_star = f(M_halo, z)
  - assumption: f(M_halo, z) is a monotonic function for M_halo
- We use:
  - Behroozi+(2013) [1207.6105]
    - calibrated by the Bolshoi simulation, complecate model
  - Moster+(2013) [1205.5807]
    - calibrated by the Millennium simulation, assuming simple double power law
  - Behroozi+(2019) [1806.07893]
    - Updated dataset and models, model selection based on Bayes factor
  - Moster+(2018) [1705.05373]
    - double-power law for efficiency evolution

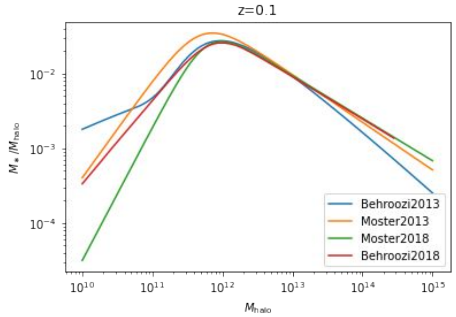

- Prior:

$$\pi_{\rm SHMR}(\rho_s, r_s, r_t) = \frac{\mathcal{N}(M_{*,\rm obs}|M_*(M_{\rm halo}), \sigma^2)\pi_{\rm satellite}(\rho_s, r_s, r_t)}{\int \mathrm{d}r_s\,\mathrm{d}\rho_s\,\mathrm{d}r_t\,\mathcal{N}(M_{*,\rm obs}|M_*(M_{\rm halo}), \sigma^2)\pi_{\rm satellite}(\rho_s, r_s, r_t)}$$

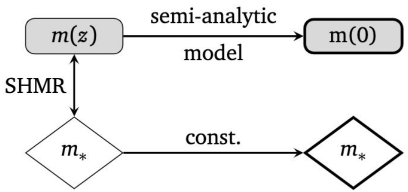

$$M_{\rm halo} \leftarrow (\rho_{s,0}, r_{s,0}, r_{t,0}) \longleftrightarrow (\rho_{s,a}, r_{s,a}, z) \xrightarrow{\rm SHMR} M_{*,a} = M_{*,0}$$

semi-analytic model in [2002.11956]

Target dSphs

- 8 classical + 26 ultrafaint dSph in [2002.11956]

Classical:

Carina
Draco
Fornax
Leo I
Leo II
Sculptor
Sextans
Ursa Minor

UFD:

Aquarius 2
Bootes I
Bootes II
Canes Venatici I
Canes Venatici II
Carina II
Coma Berenices
Draco II
Eridanus II
Grus I
Hercules
Horologium I
Hyrdus 1
Leo IV
Leo T
Leo V
Pegasus III
Pisces II
Reticulum II
Segue 1
Segue 2
Triangulum II
Tucana II
Tucana III
Ursa Major I
Ursa Major II

MCMC Analysis

- Jeans analysis
  - 6 Parameters
  - Prior choices
    - photometry only
    - photometry + satellite
    - photometry + satellite + SHMR
  - Bayesian analysis to calculate posterior probability
    - MCMC tool: `emcee 3.0.2`

parameter	min.	max.
$\log_{10} R_e/[\mathrm{pc}]$	1.0	3.5
$\log_{10} r_s/[\mathrm{pc}]$	0.0	5.0
$\log_{10} \rho_s/[M_\odot \mathrm{pc}^{-3}]$	-4.0	4.0
$\log_{10} r_t/[\mathrm{pc}]$	0.0	5.0
$-\log_{10}(1-\beta_{\mathrm{ani}})$	-1.0	1.0
$v_{\mathrm{dSph}}/[\mathrm{km\,s^{-1}}]$	-1000	1000

Results

- vs. radial independent analysis [2002.11956]
    - radial dependence of the likelihood break the degeneracy of the parameter

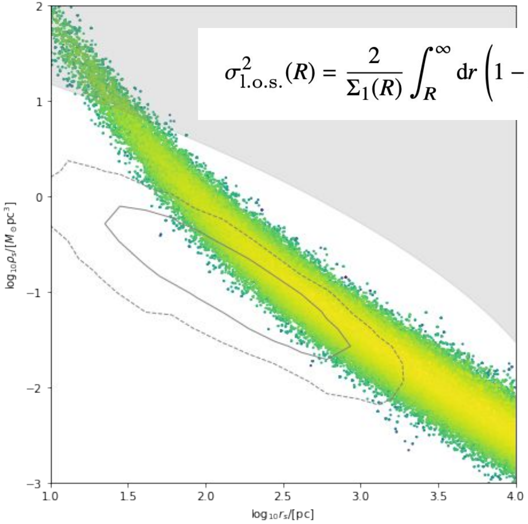

$$\sigma^2_{\mathrm{l.o.s.}}(R) = \frac{2}{\Sigma_1(R)}\int_R^\infty \mathrm{d}r\left(1-\beta_{\mathrm{ani}}\frac{R^2}{r^2}\right)\frac{\nu_1(r)\sigma_r^2(r)}{\sqrt{1-R^2/r^2}},$$

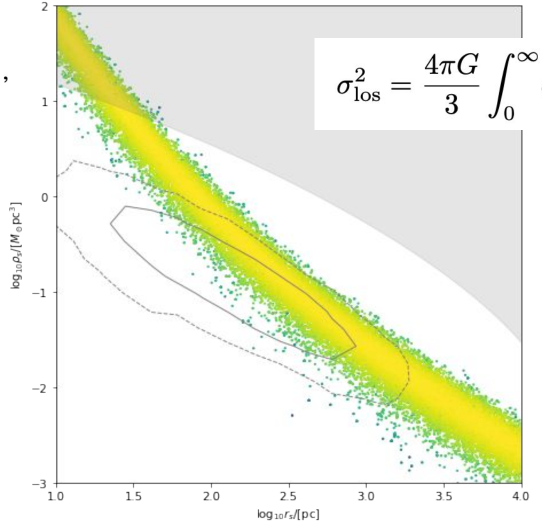

$$\sigma^2_{\mathrm{los}} = \frac{4\pi G}{3}\int_0^\infty dr\; r\nu_\star(r)M(r),$$

Results

- Posterior density function

e.g. Coma Berenices

- satellite prior only
- likelihood only
- likelihood + satellite (V_50 = 10.5 km/s)
- likelihood + satellite (V_50 = 18 km/s)
- likelihood + satellite (V_50 = 10.5 km/s) + SHMR(Behroozi)
- likelihood + satellite (V_50 = 18 km/s) + SHMR(Behroozi)
- likelihood + satellite (V_50 = 10.5 km/s) + SHMR(Moster)
- likelihood + satellite (V_50 = 18 km/s) + SHMR(Moster)

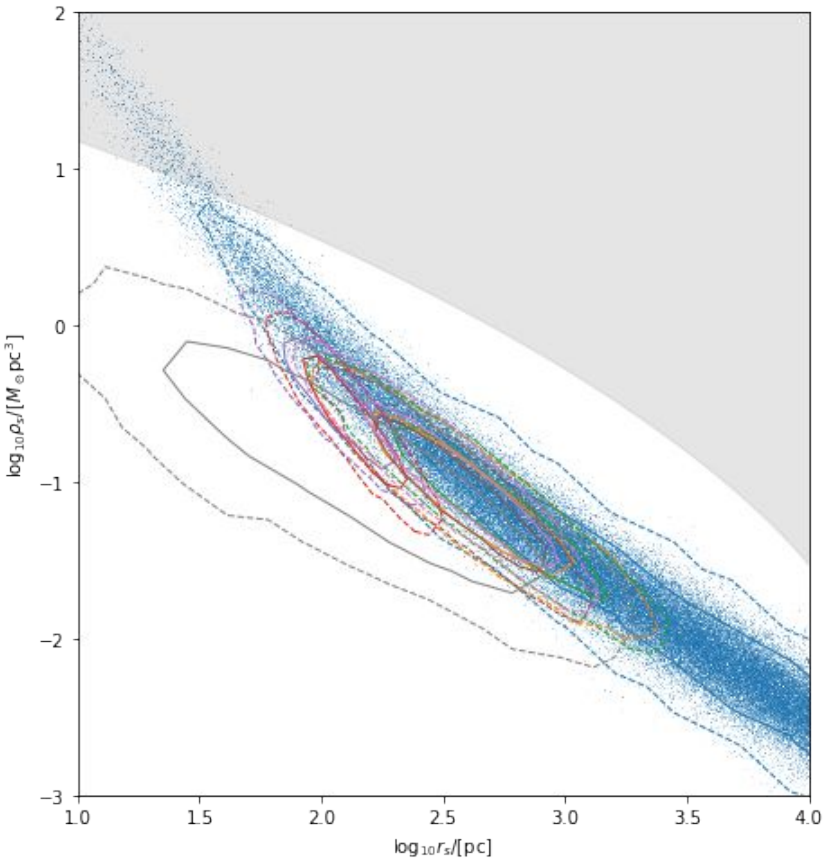

Results

- J-factor

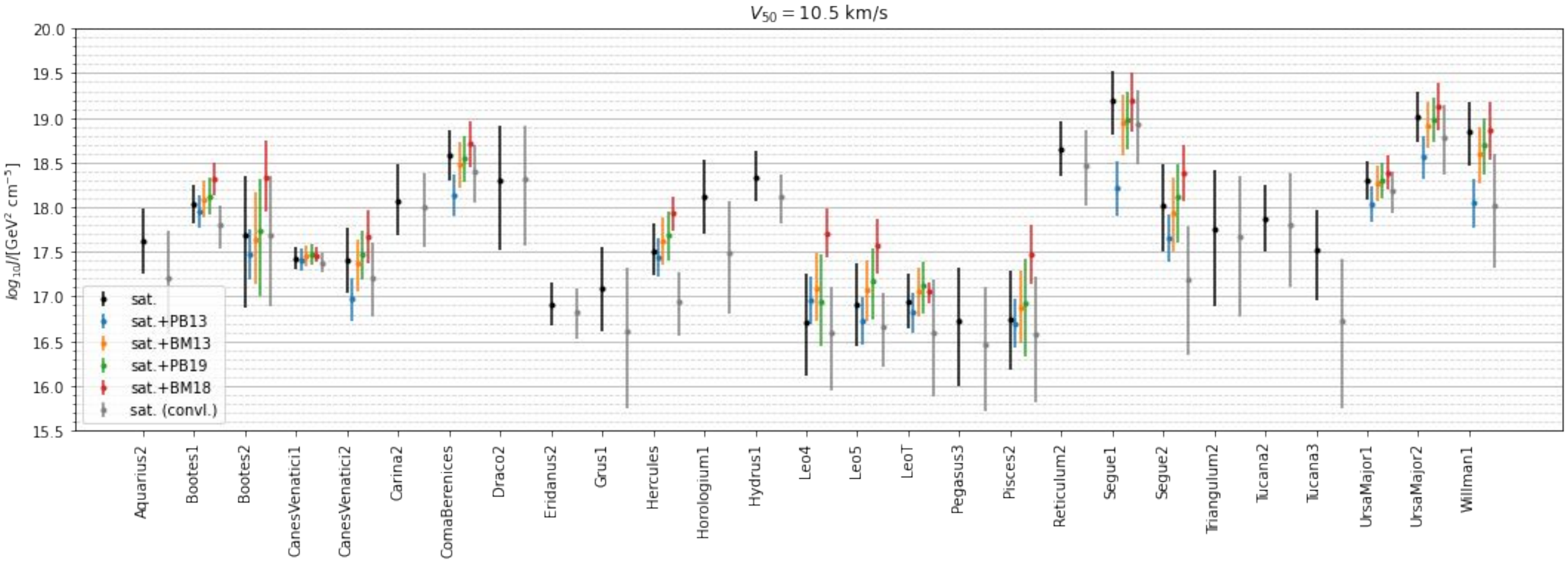

Results

- J-factor
  - slightly larger than those of the velocity independent analysis
    - radial dependence of the likelihood excludes too compact or faint DM halo having small J-factor
      - Note: anisotropy profile dependence in the velocity dispersion
  - SHMR priors can decrease J-factor uncertainty (upto ~50%) but results are model dependent
    - Test of SHMR models by using dSphs?

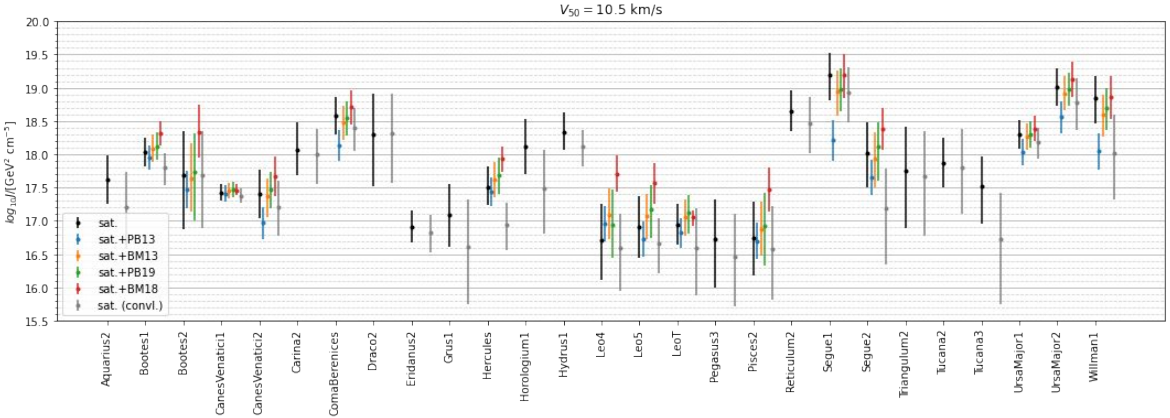

Results

- J-factors vs. Bayes factors
  - Deviated results have less Bayes factor values
    → Results of the satellite prior analysis is stable
    if we consider their Bayes factors

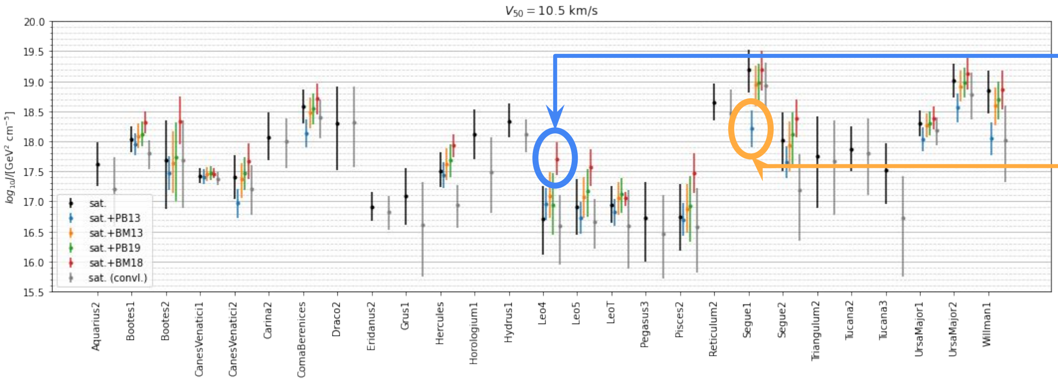

Table 6: The logarithm of Bayes factors of each model calculated according to Eq. (20). Column 1 shows the Bayes factor of sat_{18} to a reference model $\mathrm{sat}_{10.5}$ for each dSphs. Columns 2-5 shows the Bayes factors of the satellite prior and SHMR analyses to the satellite prior only analysis $\mathrm{sat}_{10.5}$ as a reference, so as Columns 6-9 not for $\mathrm{sat}_{10.5}$ but sat_{18} cases. By definition, positive (negative) values mean that the corresponding model is more (less) credible than the reference model.

	$\mathrm{sat.}_{18}/\mathrm{sat.}_{10.5}$ w/o SHMR	$\mathrm{sat.}_{10.5}$ PB13	BM13	PB19	BM18	$\mathrm{sat.}_{18}$ PB13	BM13	PB19	BM18
Aquarius2	0.77	-	-	-	-	-	-	-	-
Bootes1	-0.01	0.34	0.20	0.17	0.09	0.12	0.10	0.21	0.11
Bootes2	-0.09	0.05	0.06	-0.05	-0.16	0.07	0.04	0.01	-0.01
CanesVenatici1	0.49	0.36	0.49	0.07	0.34	0.33	-0.01	-0.31	-0.03
CanesVenatici2	1.29	-0.70	0.64	0.92	2.08	-2.61	-0.70	0.15	0.71
Carina2	-0.14	-	-	-	-	-	-	-	-
ComaBerenices	1.06	-1.71	-0.09	0.35	1.75	-3.07	-0.52	0.07	0.64
Draco2	0.16	-	-	-	-	-	-	-	-
Eridanus2	0.79	-	-	-	-	-	-	-	-
Grus1	-0.30	-	-	-	-	-	-	-	-
Hercules	0.88	0.58	0.96	0.59	1.06	-0.04	-0.06	-0.07	0.15
Horologium1	1.12	-	-	-	-	-	-	-	-
Hydrus1	-0.17	-	-	-	-	-	-	-	-
Leo4	-0.16	0.34	0.02	[illegible]	-0.93	0.44	0.15	0.01	-0.72
Leo5	-0.03	0.34	0.51	0.04	0.24	-0.47	-0.15	0.31	0.45
LeoT	1.39	0.65	1.85	1.43	0.84	-0.01	0.47	0.08	-0.61
Pegasus3	1.28	-	-	-	-	-	-	-	-
Pisces2	0.27	0.49	0.26	-0.04	-0.07	0.29	-0.01	-0.11	-0.28
Reticulum2	0.96	-	-	-	-	-	-	-	-
Segue1	[illegible]	-2.63	-1.00	-0.27	1.36	-4.29	-1.01	-0.05	-0.41
Segue2	0.08	0.11	0.12	0.21	0.26	-0.17	-0.20	0.04	-0.10
Triangulum2	-0.65	-	-	-	-	-	-	-	-
Tucana2	-0.13	-	-	-	-	-	-	-	-
Tucana3	-2.75	-	-	-	-	-	-	-	-
UrsaMajor1	1.06	-5.26	-0.16	0.61	1.84	-5.30	-0.45	-0.08	0.80
UrsaMajor2	1.25	-4.98	-1.11	0.05	1.67	-5.93	-0.63	-0.21	0.37
Willman1	2.07	-3.05	-1.05	-0.62	1.71	-4.90	-1.26	-0.37	-0.29

Summary

- dSphs play an important role of detecting dark matter by the indirect detection method, but their dark matter density are still ambiguous
- We estimate the DM density profile using velocity dependent likelihood with
    - satellite prior
    - stellar-to-halo mass relation (SHMR)
- The radial dependence of the velocity dispersion breaks the parameter degeneracy and gives more reasonable results
- SHMR priors decrease J-factor uncertainties but results have SHMR model dependence. Combining the J-factors and Bayes factors, we obtain reliable estimate of J-factor values

Backup

SHMR

- The stellar-to-halo mass relation (SHMR)
  - empirical relation between the stellar and DM halo mass of galaxies: M_star = f(M_halo, z)
  - assumption: f(M_halo, z) is a monotonic function for M_halo

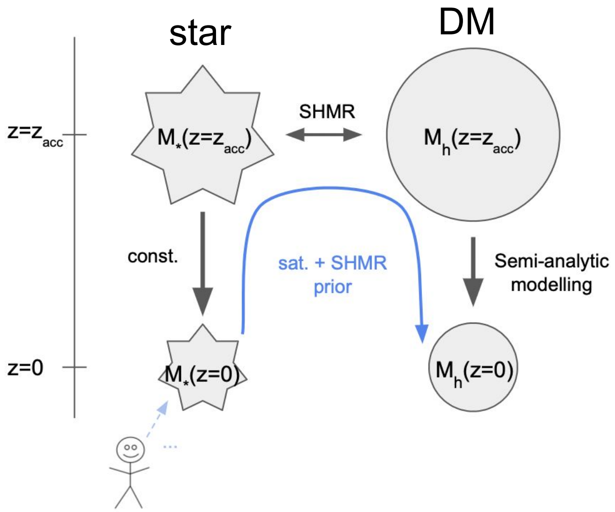

J-factors (table)

	w/o SHMR			PB13		BM13		PB19		BM18	
	flat	sat.$_{10.5}$	sat.$_{18}$	sat.$_{10.5}$	sat.$_{18}$	sat.$_{10.5}$	sat.$_{18}$	sat.$_{10.5}$	sat.$_{18}$	sat.$_{10.5}$	sat.$_{18}$
Aquarius2	$18.2^{+0.6}_{-0.6}$	$17.6^{+0.4}_{-0.4}$	$17.8^{+0.3}_{-0.4}$	-	-	-	-	-	-	-	-
Bootes1	$18.2^{+0.3}_{-0.3}$	$18.0^{+0.2}_{-0.2}$	$18.1^{+0.2}_{-0.2}$	$17.9^{+0.2}_{-0.2}$	$18.0^{+0.2}_{-0.2}$	$18.1^{+0.2}_{-0.2}$	$18.1^{+0.2}_{-0.2}$	$18.1^{+0.2}_{-0.2}$	$18.1^{+0.2}_{-0.2}$	$18.3^{+0.2}_{-0.2}$	$18.3^{+0.2}_{-0.2}$
Bootes2	$16.6^{+2.8}_{-4.9}$	$17.7^{+0.7}_{-0.8}$	$18.4^{+0.5}_{-0.5}$	$17.5^{+0.3}_{-0.3}$	$17.5^{+0.3}_{-0.3}$	$17.6^{+0.5}_{-0.5}$	$17.8^{+0.7}_{-0.7}$	$17.7^{+0.6}_{-0.7}$	$18.3^{+0.4}_{-0.4}$	$18.3^{+0.4}_{-0.4}$	$18.4^{+0.4}_{-0.4}$
CanesVenatici1	$17.6^{+0.3}_{-0.2}$	$17.4^{+0.1}_{-0.1}$	$17.5^{+0.1}_{-0.1}$	$17.4^{+0.1}_{-0.1}$	$17.4^{+0.1}_{-0.1}$	$17.5^{+0.1}_{-0.1}$	$17.4^{+0.1}_{-0.1}$	$17.5^{+0.1}_{-0.1}$	$17.5^{+0.1}_{-0.1}$	$17.5^{+0.1}_{-0.1}$	$17.5^{+0.1}_{-0.1}$
CanesVenatici2	$17.9^{+0.5}_{-0.5}$	$17.4^{+0.4}_{-0.4}$	$17.6^{+0.3}_{-0.3}$	$17.0^{+0.2}_{-0.2}$	$17.1^{+0.2}_{-0.2}$	$17.4^{+0.3}_{-0.3}$	$17.5^{+0.3}_{-0.3}$	$17.5^{+0.3}_{-0.3}$	$17.5^{+0.3}_{-0.3}$	$17.7^{+0.3}_{-0.3}$	$17.7^{+0.3}_{-0.3}$
Carina2	$18.4^{+0.6}_{-0.5}$	$18.1^{+0.4}_{-0.4}$	$18.4^{+0.4}_{-0.4}$	-	-	-	-	-	-	-	-
ComaBerenices	$19.0^{+0.3}_{-0.4}$	$18.6^{+0.3}_{-0.3}$	$18.7^{+0.3}_{-0.3}$	$18.1^{+0.2}_{-0.2}$	$18.2^{+0.2}_{-0.2}$	$18.5^{+0.2}_{-0.3}$	$18.6^{+0.2}_{-0.3}$	$18.5^{+0.3}_{-0.3}$	$18.6^{+0.2}_{-0.2}$	$18.7^{+0.3}_{-0.3}$	$18.7^{+0.3}_{-0.3}$
Draco2	$16.8^{+2.5}_{-4.8}$	$18.3^{+0.6}_{-0.8}$	$18.9^{+0.4}_{-0.5}$	-	-	-	-	-	-	-	-
Eridanus2	$17.3^{+0.4}_{-0.4}$	$16.9^{+0.3}_{-0.2}$	$17.0^{+0.2}_{-0.2}$	-	-	-	-	-	-	-	-
Grus1	$17.4^{+0.9}_{-0.9}$	$17.1^{+0.5}_{-0.5}$	$17.4^{+0.4}_{-0.4}$	-	-	-	-	-	-	-	-
Hercules	$17.9^{+0.4}_{-0.4}$	$17.5^{+0.3}_{-0.3}$	$17.7^{+0.3}_{-0.3}$	$17.4^{+0.2}_{-0.2}$	$17.5^{+0.2}_{-0.2}$	$17.6^{+0.3}_{-0.3}$	$17.6^{+0.3}_{-0.3}$	$17.7^{+0.3}_{-0.3}$	$17.7^{+0.3}_{-0.3}$	$17.9^{+0.2}_{-0.2}$	$18.0^{+0.2}_{-0.2}$
Horologium1	$19.1^{+0.7}_{-0.6}$	$18.1^{+0.4}_{-0.4}$	$18.3^{+0.3}_{-0.4}$	-	-	-	-	-	-	-	-
Hydrus1	$18.5^{+0.4}_{-0.3}$	$18.3^{+0.3}_{-0.3}$	$18.5^{+0.3}_{-0.3}$	-	-	-	-	-	-	-	-
Leo4	$15.6^{+1.9}_{-5.1}$	$16.7^{+0.5}_{-0.6}$	$17.2^{+0.5}_{-0.5}$	$17.0^{+0.3}_{-0.3}$	$17.0^{+0.3}_{-0.3}$	$17.1^{+0.4}_{-0.4}$	$17.1^{+0.4}_{-0.4}$	$16.9^{+0.5}_{-0.5}$	$17.2^{+0.4}_{-0.5}$	$17.7^{+0.3}_{-0.3}$	$17.7^{+0.3}_{-0.3}$
Leo5	$17.2^{+0.8}_{-0.8}$	$16.9^{+0.4}_{-0.5}$	$17.3^{+0.4}_{-0.4}$	$16.7^{+0.3}_{-0.3}$	$16.9^{+0.3}_{-0.3}$	$17.1^{+0.3}_{-0.3}$	$17.2^{+0.4}_{-0.4}$	$17.2^{+0.4}_{-0.4}$	$17.3^{+0.3}_{-0.4}$	$17.6^{+0.3}_{-0.3}$	$17.5^{+0.3}_{-0.3}$
LeoT	$17.6^{+0.4}_{-0.4}$	$16.9^{+0.3}_{-0.3}$	$17.0^{+0.3}_{-0.3}$	$16.8^{+0.2}_{-0.2}$	$16.9^{+0.2}_{-0.2}$	$17.1^{+0.3}_{-0.3}$	$17.1^{+0.2}_{-0.3}$	$17.1^{+0.3}_{-0.3}$	$17.1^{+0.3}_{-0.3}$	$17.1^{+0.1}_{-0.1}$	$17.1^{+0.1}_{-0.1}$
Pegasus3	$17.8^{+1.0}_{-2.1}$	$16.7^{+0.6}_{-0.7}$	$17.2^{+0.4}_{-0.5}$	-	-	-	-	-	-	-	-
Pisces2	$17.2^{+0.9}_{-1.2}$	$16.7^{+0.6}_{-0.6}$	$17.2^{+0.5}_{-0.5}$	$16.7^{+0.3}_{-0.3}$	$16.7^{+0.3}_{-0.3}$	$16.9^{+0.4}_{-0.4}$	$16.9^{+0.5}_{-0.5}$	$16.9^{+0.5}_{-0.6}$	$17.2^{+0.4}_{-0.5}$	$17.5^{+0.3}_{-0.3}$	$17.5^{+0.3}_{-0.3}$
Reticulum2	$19.0^{+0.4}_{-0.4}$	$18.7^{+0.3}_{-0.3}$	$18.8^{+0.3}_{-0.3}$	-	-	-	-	-	-	-	-
Segue1	$19.7^{+0.4}_{-0.4}$	$19.2^{+0.3}_{-0.4}$	$19.3^{+0.3}_{-0.3}$	$18.2^{+0.3}_{-0.3}$	$18.4^{+0.3}_{-0.3}$	$18.9^{+0.3}_{-0.4}$	$19.2^{+0.3}_{-0.3}$	$19.0^{+0.3}_{-0.3}$	$19.2^{+0.3}_{-0.3}$	$19.2^{+0.3}_{-0.4}$	$19.2^{+0.3}_{-0.4}$
Segue2	$18.0^{+0.7}_{-2.1}$	$18.0^{+0.5}_{-0.5}$	$18.4^{+0.4}_{-0.4}$	$17.7^{+0.3}_{-0.3}$	$17.7^{+0.3}_{-0.3}$	$17.9^{+0.4}_{-0.4}$	$18.1^{+0.4}_{-0.6}$	$18.1^{+0.4}_{-0.5}$	$18.4^{+0.3}_{-0.4}$	$18.4^{+0.3}_{-0.3}$	$18.4^{+0.3}_{-0.3}$
Triangulum2	$14.4^{+2.9}_{-3.9}$	$17.7^{+0.7}_{-0.9}$	$18.5^{+0.4}_{-0.5}$	-	-	-	-	-	-	-	-
Tucana2	$18.1^{+0.6}_{-0.5}$	$17.9^{+0.4}_{-0.4}$	$18.2^{+0.4}_{-0.4}$	-	-	-	-	-	-	-	-
Tucana3	$15.7^{+1.8}_{-4.3}$	$17.5^{+0.5}_{-0.6}$	$18.1^{+0.3}_{-0.3}$	-	-	-	-	-	-	-	-
UrsaMajor1	$18.7^{+0.3}_{-0.3}$	$18.3^{+0.2}_{-0.2}$	$18.3^{+0.2}_{-0.2}$	$18.0^{+0.2}_{-0.2}$	$18.1^{+0.2}_{-0.2}$	$18.3^{+0.2}_{-0.2}$	$18.3^{+0.2}_{-0.2}$	$18.3^{+0.2}_{-0.2}$	$18.3^{+0.2}_{-0.2}$	$18.4^{+0.2}_{-0.2}$	$18.4^{+0.2}_{-0.2}$
UrsaMajor2	$19.5^{+0.4}_{-0.4}$	$19.0^{+0.3}_{-0.3}$	$19.1^{+0.2}_{-0.2}$	$18.6^{+0.2}_{-0.2}$	$18.6^{+0.2}_{-0.2}$	$18.9^{+0.3}_{-0.3}$	$19.1^{+0.3}_{-0.3}$	$19.0^{+0.2}_{-0.2}$	$19.0^{+0.3}_{-0.2}$	$19.1^{+0.3}_{-0.3}$	$19.1^{+0.3}_{-0.3}$
Willman1	$19.5^{+0.4}_{-0.4}$	$18.8^{+0.3}_{-0.4}$	$19.0^{+0.3}_{-0.3}$	$18.0^{+0.3}_{-0.3}$	$18.1^{+0.3}_{-0.3}$	$18.6^{+0.3}_{-0.3}$	$18.9^{+0.3}_{-0.3}$	$18.7^{+0.3}_{-0.3}$	$18.8^{+0.3}_{-0.3}$	$18.9^{+0.3}_{-0.3}$	$18.9^{+0.3}_{-0.3}$

	w/o SHMR		SHMR$_{\text{Moster}}$	SHMR$_{\text{Behroozi}}$
	flat	sat.	sat.	sat.
Carina	$17.9^{+0.1}_{-0.1}$	$17.9^{+0.1}_{-0.1}$	$17.9^{+0.1}_{-0.1}$	$17.9^{+0.1}_{-0.1}$
Draco	$18.9^{+0.1}_{-0.1}$	$18.9^{+0.1}_{-0.1}$	$18.9^{+0.1}_{-0.1}$	$18.8^{+0.1}_{-0.1}$
Fornax	$17.9^{+0.2}_{-0.1}$	$18.0^{+0.1}_{-0.1}$	$18.0^{+0.1}_{-0.1}$	$18.0^{+0.1}_{-0.1}$
Leo1	$17.8^{+0.2}_{-0.1}$	$17.7^{+0.1}_{-0.1}$	$17.7^{+0.1}_{-0.1}$	$17.7^{+0.1}_{-0.1}$
Leo2	$17.8^{+0.2}_{-0.2}$	$17.7^{+0.2}_{-0.1}$	$17.7^{+0.2}_{-0.1}$	$17.6^{+0.1}_{-0.1}$
Sculptor	$18.6^{+0.1}_{-0.0}$	$18.5^{+0.0}_{-0.0}$	$18.6^{+0.0}_{-0.0}$	$18.5^{+0.0}_{-0.0}$
Sextans1	$18.1^{+0.4}_{-0.2}$	$18.1^{+0.1}_{-0.1}$	$18.1^{+0.1}_{-0.1}$	$18.1^{+0.1}_{-0.1}$
UrsaMinor	$18.5^{+0.1}_{-0.1}$	$18.5^{+0.1}_{-0.1}$	$18.5^{+0.1}_{-0.1}$	$18.5^{+0.1}_{-0.1}$

J-factors

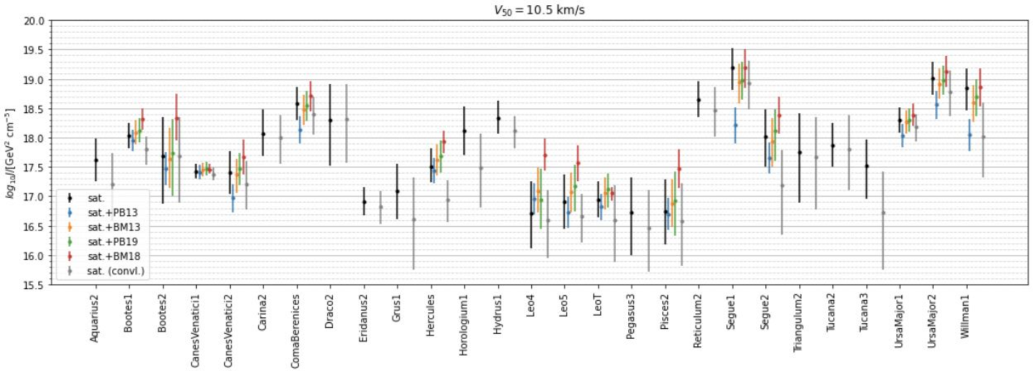
$V_{50} = 10.5$ km/s
$log_{10}J/[\mathrm{GeV}^2\ \mathrm{cm}^{-5}]$
sat.
sat.+PB13
sat.+BM13
sat.+PB19
sat.+BM18
sat. (convl.)
Aquarius2
Bootes1
Bootes2
CanesVenatici1
CanesVenatici2
Carina2
ComaBerenices
Draco2
Eridanus2
Grus1
Hercules
Horologium1
Hydrus1
Leo4
Leo5
LeoT
Pegasus3
Pisces2
Reticulum2
Segue1
Segue2
Triangulum2
Tucana2
Tucana3
UrsaMajor1
UrsaMajor2
Willman1

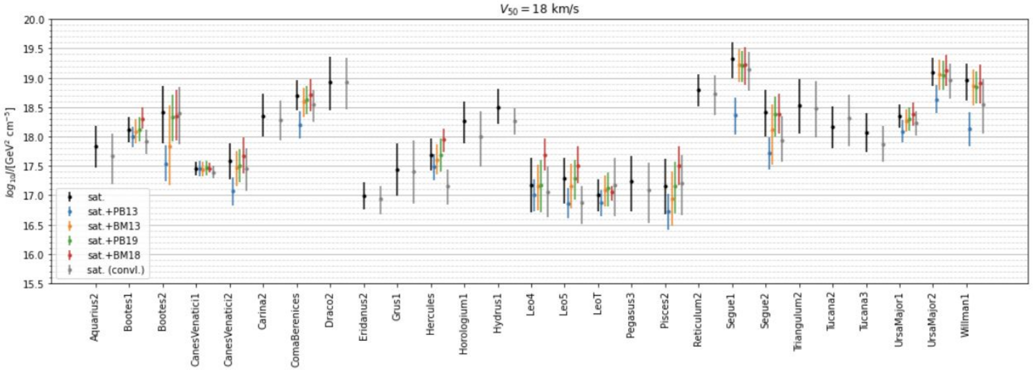
$V_{50} = 18$ km/s
$log_{10}J/[\mathrm{GeV}^2\ \mathrm{cm}^{-5}]$
sat.
sat.+PB13
sat.+BM13
sat.+PB19
sat.+BM18
sat. (convl.)
Aquarius2
Bootes1
Bootes2
CanesVenatici1
CanesVenatici2
Carina2
ComaBerenices
Draco2
Eridanus2
Grus1
Hercules
Horologium1
Hydrus1
Leo4
Leo5
LeoT
Pegasus3
Pisces2
Reticulum2
Segue1
Segue2
Triangulum2
Tucana2
Tucana3
UrsaMajor1
UrsaMajor2
Willman1

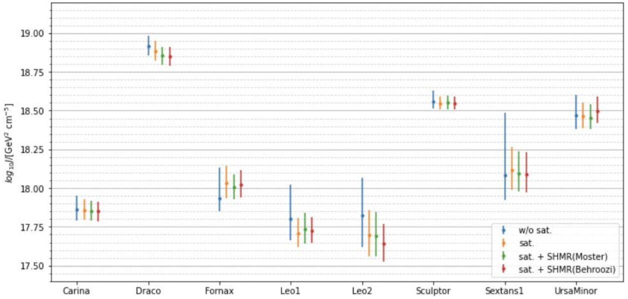
$log_{10}J/[\mathrm{GeV}^2\ \mathrm{cm}^{-5}]$
w/o sat.
sat.
sat. + SHMR(Moster)
sat. + SHMR(Behroozi)
Carina
Draco
Fornax
Leo1
Leo2
Sculptor
Sextans1
UrsaMinor

Difference of Jeans analyses

- [2002.11956]: velocity dispersion averaged over total system

$$\sigma_{\rm los}^2 = \frac{4\pi G}{3}\int_0^\infty dr\; r\nu_\star(r)M(r),$$

- This work: radial dependent velocity dispersion calculated by the spherical Jeans equation

$$\sigma_{\rm l.o.s.}^2(R) = \frac{2}{\Sigma_1(R)}\int_R^\infty {\rm d}r\left(1-\beta_{\rm ani}\frac{R^2}{r^2}\right)\frac{\nu_1(r)\sigma_r^2(r)}{\sqrt{1-R^2/r^2}}\;,$$

Models

- Plummer model

$$\nu(r) = \frac{3}{4\pi R_e^3}\left(1 + \left(\frac{r}{R_e}\right)^2\right)^{-5/2},$$

$$\Sigma(R) = \frac{1}{\pi}\left(1 + \frac{R^2}{R_e^2}\right)^{-2},$$

- Truncated NFW model
  - Outermost halo is striped by tidal force

$$\rho(r) = \begin{cases} \rho_s\left(\frac{r}{r_s}\right)^{-1}\left(1 + \frac{r}{r_s}\right)^{-2} & (0 \le r \le r_t) \\ 0 & (r_t < r) \end{cases},$$

$$M(r) = \begin{cases} 4\pi\rho_s r_s^3\left(\log\left(1 + \frac{r}{r_s}\right) - \frac{r}{r+r_s}\right) & (0 \le r \le r_t) \\ 4\pi\rho_s r_s^3\left(\log\left(1 + \frac{r_t}{r_s}\right) - \frac{r_t}{r_t+r_s}\right) & (r_t < r), \end{cases}$$

dSphs and DM detection

- Dwarf spheroidal galaxies (dSphs)
  - inner DM halo profile gives constraints on DM self-interaction

e.g. Fornax dSph

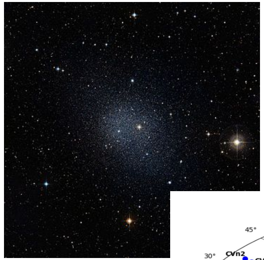

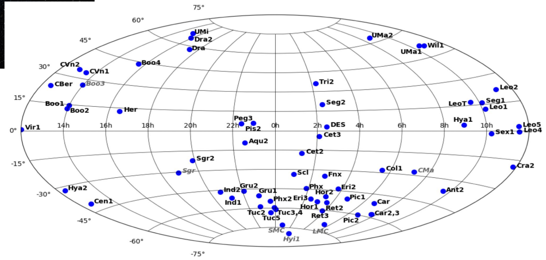

McConachie et al. [2007.05011]

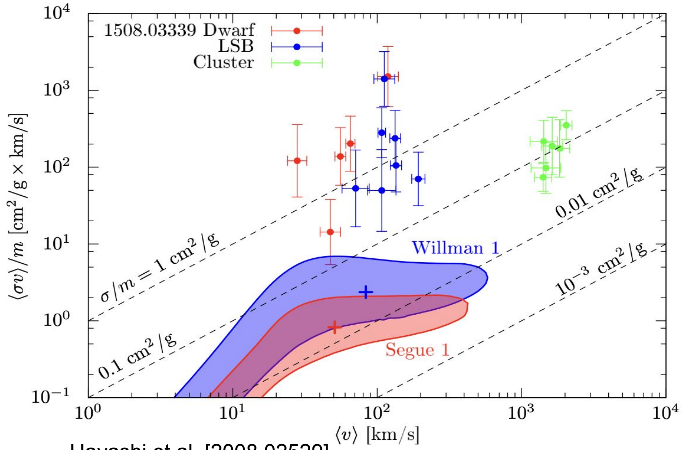

Hayashi et al. [2008.02529]

Sommerfeld effect

- Sommerfeld effect:
    - nonrelativistic effect of scattering

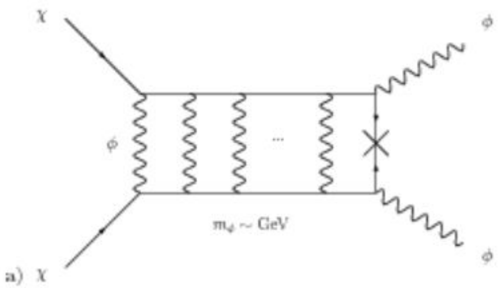

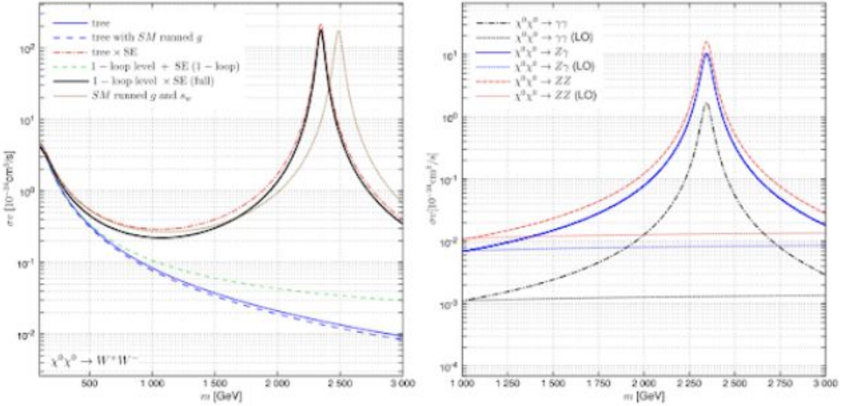

Difference of SHMRs

-

For low-mass haloes ($M_h < 10^{11}$ M$_\odot$), the best-fitting model has a weaker upturn in the SMHM ratio than found by Behroozi et al. (2013e); this is because Behroozi et al. (2013e) assumed a strong surface-brightness incompleteness correction for faint galaxies that is no longer observationally supported (Williams et al. 2016). This will make it easier to reconcile observed galaxy counts with the HI mass function and observed HI gas fractions in faint galaxies (Popping et al. 2015).

The SMHM relation for star-forming vs. quiescent galaxies depends on the correlation between galaxy and halo assembly (§4.2) and the evolution of the SMHM relation (see also Moster et al. 2018). As shown in Fig. 38, there remain significant differences across studies (see also Wechsler & Tinker 2018). Our model is flexible in terms of both the SMHM relation evolution and the galaxy–halo assembly correlation, and suggests that the stellar mass–halo mass relation at fixed halo mass is similar for star-forming and quiescent central galaxies, matching the conclusion in Zu & Mandelbaum (2016). The results of Moster et al. (2018) and Rodríguez-Puebla et al. (2015) give opposite conclusions of higher and lower (respectively) median stellar masses for quiescent compared to star-forming galaxies, despite using the same underlying data (correlation functions in the SDSS) to constrain their models. In part, these divergent conclusions arise because correlation functions and weak lensing measurements are both very sensitive to satellite clustering; hence, small changes to the satellite halo occupation can lead to large changes in the inferred occupation for central galaxies. Applying a cut to first remove satellites before measuring clustering, environment, or lensing (as in both this study and Zu & Mandelbaum 2016) is hence necessary to robustly determine SMHM differences for star-forming and quiescent central galaxies. As noted in Zu & Mandelbaum (2016) and Moster et al. (2018), having an equivalent median stellar mass at fixed halo mass does *not* imply that the median halo mass at fixed stellar mass will be equal for star-forming and quiescent galaxies. Because the ratio of star-forming to quiescent galaxies drops rapidly with increasing halo mass, it is much more likely in this case that a given massive star-forming galaxy will be hosted by a lower-mass halo than a massive quiescent galaxy.

Behroozi+(2019) [1806.07893]